energy&fuels

ARTICLE

pubs.acs.org/EF

Behavior of Alkali Metal Hydroxides/Chlorides for NO Reduction in a Biomass Reburning Process

Sen Li* and Xiaolin Wei

Institute of Mechanics, Chinese Academy of Sciences, Number 15 Beisihuanxi Road, Beijing 100190, People's Republic of China

ABSTRACT: The behaviors of alkali metal hydroxides and chlorides released from biomass for NO reduction during biomass reburning were analyzed. Na-Containing species have great promotion of NO reduction by controlling the free radicals of H and OH, as compared to K-containing species, and the effects of alkali metal hydroxide vapors and alkali metal chloride vapors on the NO reduction rate were identical. At the beginning stage of biomass reburning, Na-containing species can effectively inhibit the conversion of HCN into NH, HNO, and N by controlling the formation of H and OH, and it avoids NO formation. At the later stage of biomass reburning, the free-radical levels of H and OH reach equilibrium, Na-containing species can promote the formation of H and OH to sustain a relatively high level through the chemical reaction path of NaOH → Na → NaOH, and NO is effectively reduced. Because the reaction rate constant of K + OH = KOH is only $^1/_{64}$ of Na + OH = NaOH, KOH has low promotion of NO reduction, as compared to NaOH.

1. INTRODUCTION

Coal combustion generates significant quantities of nitrogen oxides (NO_x), leading to the formation of both acid precipitation and photochemical smog.[1] In recent years, some new combustion technologies have been developed for clean and efficient combustion.[2] Reburning is one of the most promising combustion modification technologies for low-cost NO_x control, and the reburning fuel can be the same as the primary fuel or a different fuel (such as coal, biomass, gas, or fuel oil).[1−10] Experiments demonstrated that biomass reburning can result in substantial NO_x reductions.[5,6,11] High-volatile biomass used as burning fuel releases a large amount of the reducing agents of NO_x to significantly reduce NO_x to N_2 in the reburning zone.

Experiments have found that the NO_x reduction rate could be improved 30% by adding NaOH into a urea solution in the process of selected noncatalytic reduction.[12,13] Liu et al.[14] have investigated the effects of sodium additives on the release of coal nitrogen on a thermogravimetric analyzer using Yibin coal from China. It was found that sodium compounds could reduce the release of NO and HCN remarkably, and sodium chloride (NaCl) had a better effect on NO reduction than sodium carbonate (Na_2CO_3). Avelina et al.[15] have found that NO reduction by potassium (K)-containing briquettes was enhanced by the presence of oxygen.

Biomass has relatively high contents of alkali metals (Na and K), and Na and K can be released in the form of alkali metal hydroxides and chlorides (e.g., KOH, NaOH, KCl, and NaCl) during biomass combustion.[3,16] During biomass combustion, the release of mineral compositions of biomass fuel is generally complex and difficult to quantitatively determine. It was found that alkali metals were released in the form of chlorides, hydroxides, and cyanates,[17−19] and these gaseous alkali metal hydroxides and chlorides could affect NO formation when biomass is used as a reburning fuel.

Biomass reburning for NO reduction may require a more complete understanding of the chemical reaction pathway of NO reduction. The goal of this paper is to gain a better understanding of the promotion mechanisms of gaseous alkali metal hydroxides and chlorides released from biomass for NO reduction in the process of biomass reburning. Biomass reburning was simulated using the Sandia SENKIN program, and the promotion mechanisms and behaviors of Na- or K-containing species for NO_x reduction were analyzed.

2. KINETIC MODEL

Because biomass has high volatile content, it is assumed that the contribution of char combustion to NO reduction is less than that of gas-phase reactions.[4] Thus, in the simulation of biomass reburning, biomass is represented as gasification products.

The chemical kinetic behavior of reactants was modeled with the Sandia SENKIN program of CHEMKIN subroutines.[19,20] The program solves the conservation equations for mass and energy, and it can calculate the temporal evolution of mole fractions of species for a homogeneous mixture in a closed reactor. The SENKIN model is appropriate to investigate the promotion mechanisms of gaseous alkali metal species for NO reduction in the process of biomass reburning in a closed chamber. The reaction pathway flux analysis is performed using MixMaster, which is based on a conserved scalar approach to reaction fluxes.[21]

The reaction mechanism is an extension of the reduction of NO by natural gas and simple hydrocarbons (C1−C4) in biomass reburning conditions.[22−25] The absent reactions of sodium, potassium, and chlorine are selected from refs 26−28 and incorporated into the mechanism, and the mechanism includes 1112 reversible reactions and 181 species. The reaction mechanisms of the NO reduction by natural gas and simple hydrocarbons (C1−C4) are documented in ref 25, and the mechanisms

Received: April 30, 2011
Revised: July 7, 2011
Published: July 11, 2011

Table 1. Fuel Analysis Properties of Furniture Waste Used as Reburning Fuel[4]

proximate analysis (wt %, as air dried)				
moisture	ash	volatile	fixed carbon	HHV (kJ kg^{-1})
6.37	1.31	79.06	19.63	20602

ultimate analysis (wt %, as air dried)						
carbon	hydrogen	oxygen	nitrogen	sulfur	ash	chlorine
53.91	6.07	38.12	0.56	0.03	1.31	0.19

ash analysis (wt %, as air dried)									
SiO_2	Al_2O_3	K_2O	Na_2O	P_2O_5	SO_3	Fe_2O_3	CaO	MgO	others
13.86	3.29	7.50	11.16	2.20	6.37	8.25	24.10	3.00	34.13

Table 2. Gasification Production Compositions of Furniture Waste (vol %)[26]

CO	C_2H_6	C_2H_4	HCN
68.86	27.40	2.60	1.10

involving sodium, potassium, and chlorine are documented in refs 27 and 28.

The mechanism of the reduction of NO_x by natural gas and simple hydrocarbons (C1−C4) in simulated reburning conditions has been extensively validated by experimental data of biomass gas NO_x reburning in refs 22−26, and the submechanism involving species containing sodium, potassium, and chlorine has been validated by the experimental data of alkali metals for NO_x reduction in the biomass reburning and combustion process.[26−29] The experiments of promotion of NO reduction by gaseous alkali metal hydroxides and chlorides released from biomass in the process of biomass reburning are few. It is difficult to validate the combined mechanisms for NO_x reduction. The combined mechanism may not quantitatively investigate the promotion effects of gaseous alkali metals on NO_x reduction, but it still effectively provides insight into the mechanisms and reaction pathways of the promotion of NO reduction by alkali metal elements released from biomass.

3. SIMULATION CONDITIONS

In the simulation of biomass reburning for NO reduction using the Sandia SENKIN model, an adiabatic system at constant pressure and temperature (P = 1.01 bar and T = 1700 K) is used to model the NO reduction process in the reburning zone, and the residence time of gas reactions is 0.4 s.

GE Energy and Environmental Research Corporation has conducted an experiment of biomass reburning to demonstrate the biomass reburning technology in a 300 kW boiler simulator facility (BSF).[4] The main fuel in the primary combustion zone was bituminous Illinois coal, and reburning fuels in the reburning zone were furniture waste pellets.

In the simulation, furniture waste is selected as reburning fuel, and the properties are presented in Table 1. The experiment demonstrated that furniture waste used as reburning fuel has a high capacity of NO reduction.[26] Experimental data results suggested that the time scale of biomass gasification under these test conditions was smaller than the characteristic time of the mixing process in the reburning zone.[4] The compositions of biomass gasification products are shown in Table 2.

Table 3. Initial Compositions of the Gas Mixture in the Simulation (vol %)[26]

CO_2	CO	C_2H_6	C_2H_4	HCN	H_2O	N_2	O_2	NO
14.93	3.13	0.86	0.12	0.05	7.79	71.27	1.85	0.004

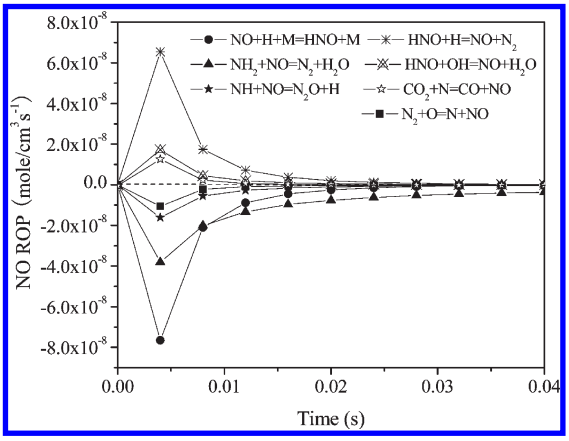

Figure 1. Rates of NO production of reactions versus the reactor time without the release of alkali metals.

The simplification of biomass gasification products is a requirement, and it is often used in computational fluid dynamic (CFD) modeling.[30,31]

The experiment conditions were a primary zone stoichiometric ratio (SR) of 1.10, a final SR of 1.15, and reburn fuel injected at a combustion gas temperature of about 1700 K, with 15% reburning heat input.[4] On the basis of the above experimental conditions, it is assured that the combustion of pulverized coal is complete in the primary combustion zone. The concentrations of gas coming from the primary combustion zone are calculated as follows: 1.8% O_2, 15.6% CO_2, 74.4% N_2, and 8.1% H_2O. The biomass entering the reburning zone can be instantaneously gasified. The gasification products completely mix with flue gas coming from the primary combustion zone, and the initial compositions of the gas mixture in the simulation are shown in Table 3. NO entering the reburning zone in the experiment varied from 400 to 900 ppm,[4] and it is given at 400 ppm in the simulation.

The available information does not allow one to identify the concentrations of alkali-metal-containing species released from the biomass to the gas phase, and it is assumed that K and Na species can be released in the vapor forms of hydroxides (KOH and NaOH) and chlorides (KCl and NaCl). In accordance with the content of K and Na in furniture waste, the maximum vapor concentration of alkali metal hydroxide or chloride is 28 ppm in the initial gas mixture.

4. SIMULATION RESULTS AND DISCUSSION

4.1. NO Reduction by Biomass Reburning without the Release of Alkali Metals. To analyze the effect of alkali metal hydroxides/chlorides on NO in the process of biomass reburning, the chemical reaction pathways of N-containing species are first presented without the release of alkali metal hydroxides/chloride.

An alternative method for the study of the relevance of the reactions is the rate of production (ROP) analysis, and it is a classic method for the identification of important reaction pathways. Thus, the rates of NO production reactions are calculated, and the top seven NO production reaction rates are presented in Figure 1. When the reaction time is greater than 0.04 s,

NO production reaction rates are very stable and approach constants, and then these rates are not provided in Figure 1 when the reaction time varies from 0.04 to 0.4 s. Figure 1 indicates that NO production rates noticeably vary at the beginning time (0−0.01 s). The reaction HNO + H = NO + N_2 plays the greatest role in NO formation, and the reaction NO + H + M = HNO + M plays the greatest role in NO reduction. The free radicals of H, OH, NH, NH_2, N, and O are important for the most important reactions involving NO production shown in Figure 1, and the concentration profiles of these radicals are depicted in a logarithmic scale, as shown in Figure 2. At the beginning stage (reaction time of 0−0.04 s) in Figure 2, free-radical concentrations vary rapidly, the concentrations of HCN, OH, H, and NH_3 are high, and the concentrations of NO, HCN, and NH_3 decrease with the reaction time. At the later stage (reaction time > 0.04 s), the free-radical concentrations are kept relatively steady. Thus, the beginning stage (reaction time of 0−0.04 s) is crucial to NO reduction during biomass reburning.

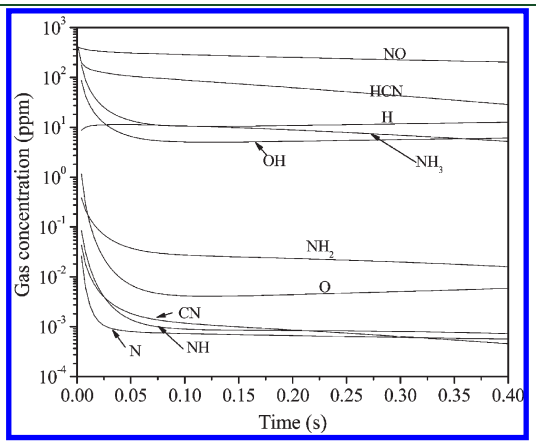

Figure 2. N-Containing species concentrations versus the residence time without the release of alkali metals.

To investigate NO reaction mechanisms, the reaction pathway flux analysis is performed using MixMaster (a Python program that is part of the Cantera suite), and the integral path analysis is based on a conserved scalar approach to reaction fluxes.[32] Figure 3 illustrates the detailed reaction pathway diagram for N-containing species during biomass at t = 0.004 s, where the relative width of the arrows indicates pathway importance. Figure 3 indicates that NO is reduced into N_2 mainly by NH_2,

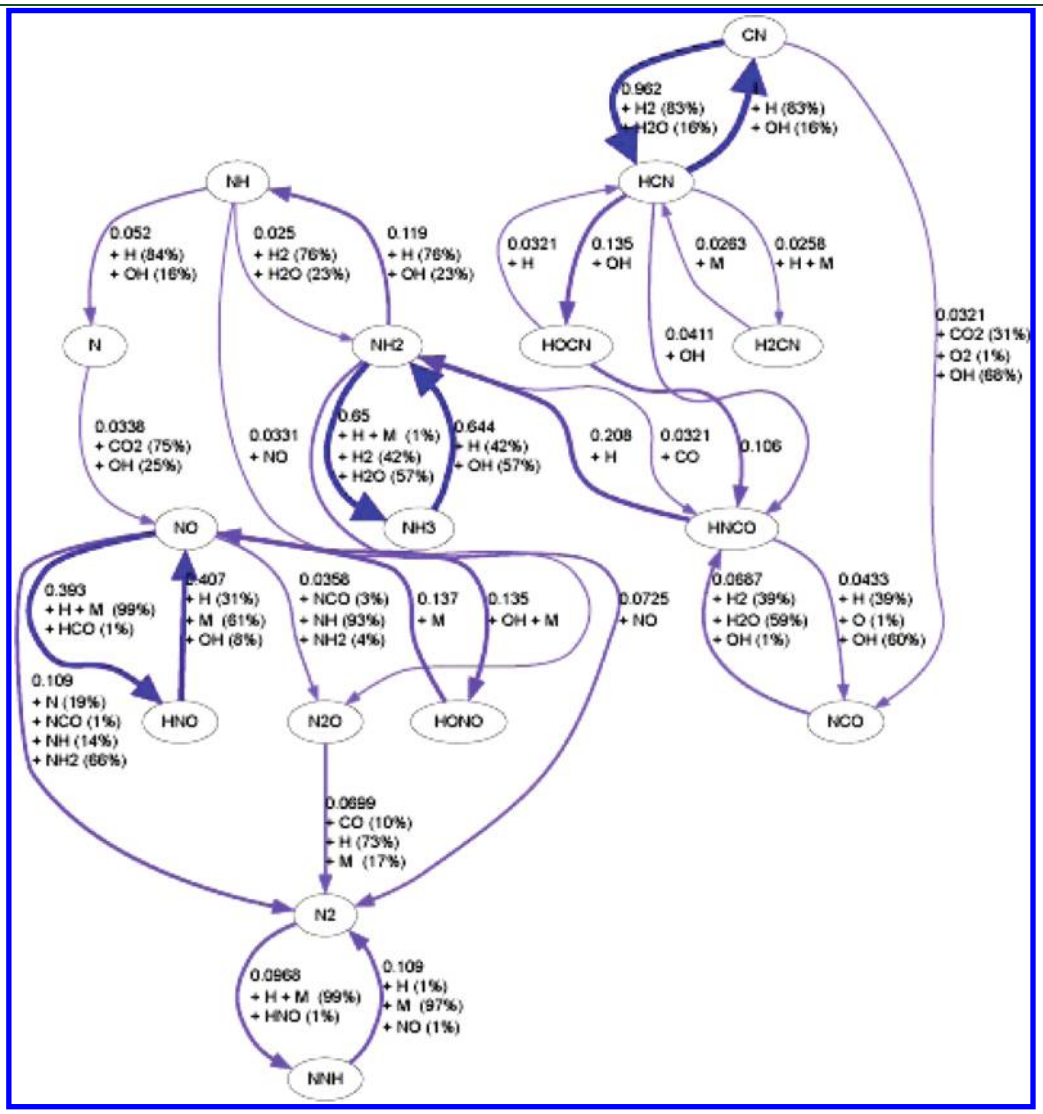

Figure 3. Reaction pathway diagram for N-containing species during biomass reburning at 0.004 s without the release of alkali metals.

dx.doi.org/10.1021/ef200661x |*Energy Fuels* 2011, 25, 3465–3475

NH, and N. The contributions of NH_2, NH, and N for NO reduction are 66, 14, and 19%, respectively. NO-Reducing agents all derive from HCN (HCN → HOCN/HNCO → NH_2 → NH → N), and H and OH play a great role in the process. The detailed pathways of NO reduction are as follows:

(1) The detailed pathway of NO reduction by NH_2.

$$HCN + OH \rightarrow HOCN + H \quad (R1)$$

$$HCN + OH \rightarrow HNCO \quad (R2)$$

$$HOCN \rightarrow HNCO \quad (R3)$$

$$HNCO + H \rightarrow NH_2 + CO \quad (R4)$$

$$NH_2 + NO \rightarrow N_2 + H_2O \quad (R5)$$

(2) The detailed pathway of NO reduction by NH.

$$NH_2 + OH \rightarrow NH + H_2O \quad (R6)$$

$$NH_2 + H \rightarrow NH + H_2 \quad (R7)$$

$$NH + NO \rightarrow N_2 + OH \quad (R8)$$

(3) The detailed pathway of NO reduction by N.

$$NH + H \rightarrow N + H_2 \quad (R9)$$

$$NH + OH \rightarrow N + H_2O \quad (R10)$$

$$N + NO \rightarrow N_2 + O \quad (R11)$$

The reaction pathway diagram also shows that NO can be produced by the following reaction pathways:

(1) NO formation through the reaction of N with CO_2 and OH.

$$N + CO_2 \rightarrow NO + CO \quad (R12)$$

$$N + OH \rightarrow NO + H \quad (R13)$$

(2) NO formation through the reaction of HNO with OH and H.

$$NH + OH \rightarrow HNO + H \quad (R14)$$

$$HNO + OH \rightarrow NO + H_2O \quad (R15)$$

$$HNO + H \rightarrow NO + H_2 \quad (R16)$$

$$HNO + M \rightarrow NO + H + M \quad (R17)$$

As known from the above analysis, the reaction pathways of N-containing species are complicated. The free radicals of NH_2, NH, N, and HNO all derive from HCN, where OH and H are intermediates at different stages, and these free radicals can not only reduce NO by R1−R11 but also produce NO by R12−R17. The net effects of NH_2 and NH are NO reduction, and the net effects of N and HNO are NO formation. As known from Figure 1, the net rates of NO reduction by NH_2 and NH are 3.81×10^{-8} and 1.61×10^{-8} mol cm^{-3} s^{-1}, respectively, and the net rates of NO formation by N and HNO are 1.68×10^{-8} and 0.61×10^{-8} mol cm^{-3} s^{-1}, respectively. Because the reaction rate constant of R5 is greater than that of R8, NO can be easily reduced by R5. NO reduction is dominated by the reaction $NH_2 + NO \rightarrow N_2 + H_2O$.

High levels of OH and H can promote NH_2 formation to easily reduce NO into N_2, but too high levels of OH and H always make NH_2 further conversed into NH, N, and HNO (see Figure 3), whose reaction rate constants of NO reduction are lower, as compared to that of NH_2. Thus, the appropriate concentrations of H and OH are very important for NO reduction during biomass reburning at the beginning stage of biomass reburning (reaction time of 0−0.04 s).

Dryer et al.[33,34] have studied the oxidation of wet CO and found that wet CO oxidation occurred predominantly by the reaction CO + OH → CO_2 + H and OH was 2 orders of magnitude greater than its equilibrium value. Such super-equilibrium concentrations of free radicals are quite normal in combustion chemistry at the initial combustion stage. When CO becomes exhausted, the ability of combustion reactions to sustain super-equilibrium concentrations of free radicals decreases and the free-radical concentrations fall toward their equilibrium values at some point.[33,34] Practical combustion demonstrated that the fast radical formation reactions and the relatively slow radical recombination reactions give rise to large super-equilibrium concentrations of O, H, and OH in the flame front zone and the equilibrium concentrations is often in the post-flame zone.[35]

On the basis of the above analysis, at the initial combustion stage, the super-equilibrium concentrations of free radicals are important for NO formation. High levels of H and OH because of CO oxidation at the initial stage make HCN conversed into not only NH_2 but also NH, N, and HNO. The reaction rate of NO reduction by NH is less than that by NH_2, and N and HNO can easily produce NO. Thus, high levels of H and OH are not conducive to NO reduction at the initial stage of biomass reburning.

Figure 4 shows the reaction pathway diagram for N-containing species at a later stage of biomass reburning (t = 0.2 s). The pathway is similar to that at the initial stage (see Figure 3), and NH_2 contribution increases by 21%, as compared to that at 0.004 s. As known from Figure 2, at t > 0.04 s, the free-radical concentrations of NH_2, NH, and N are very low, which makes the NO reduction rate decrease. Because the O_2 concentration is low during reburning, the oxidation of combustible species can be inhibited by oxygen exhaustion. The concentrations of H and OH fall toward their equilibrium values (see Figure 2). The low levels of H and OH are not conducive to the formation of NO-reducing agents. NO reduction rates are approximate to 0, except for R5, and then the NO concentration slowly decreases with the reaction time (see Figure 2).

In other words, during biomass reburning without the release of alkali metals, NO cannot effectively reduce NO because of super-equilibrium levels of H and OH at the beginning stage and too low levels of H and OH at the later stage.

4.2. NO Reduction by the Release of Alkali Metal Hydroxides. To investigate the influence of alkali metal hydroxide vapor on NO reduction during biomass reburning, the NO reduction rate is defined as

$$\Delta\eta = \frac{C_{1,NO} - C_{2,NO}}{C_{0,NO}} \times 100\% \quad (1)$$

where $C_{0,NO}$ is the initial concentration of NO (400 ppm) in the gas mixture in the simulation, as shown in Table 3, $C_{1,NO}$ is the NO emission concentration in the absence of alkali metal vapor,

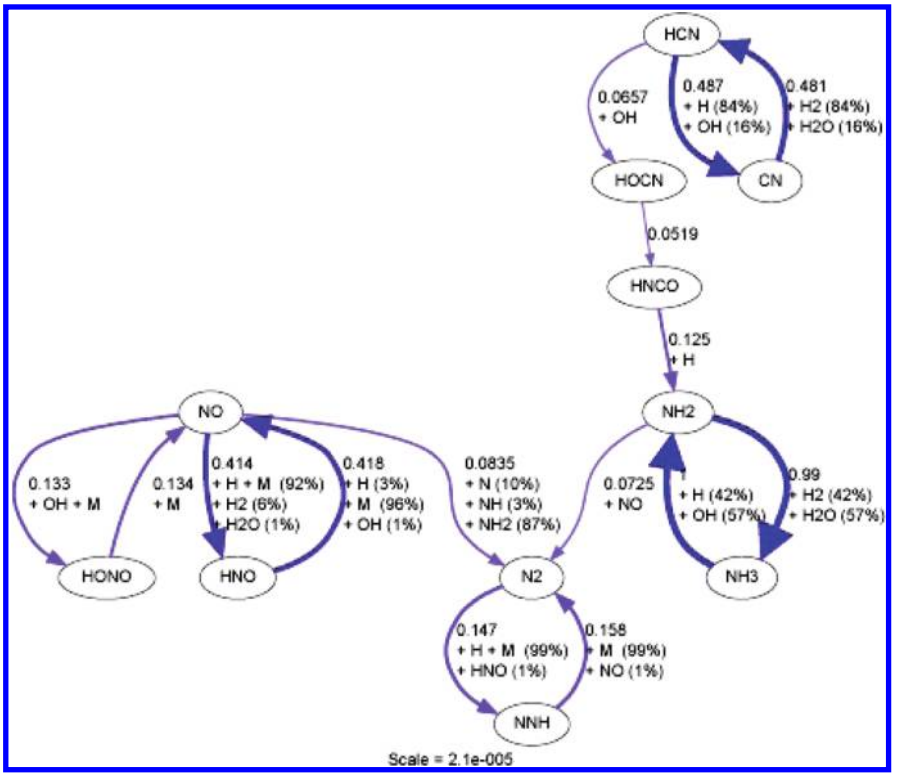

Figure 4. Main reaction pathway diagram for N-containing species during biomass reburning at 0.2 s without the release of alkali metals.

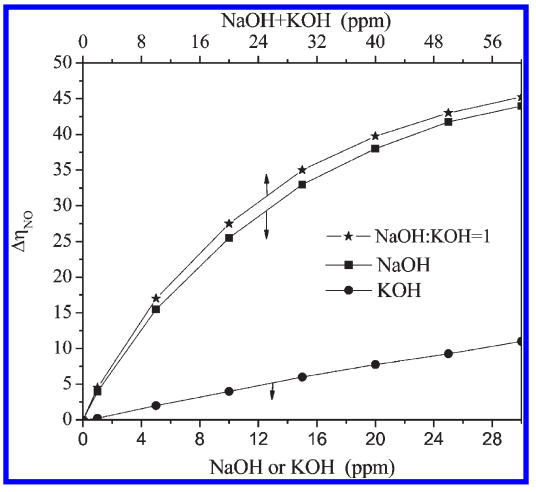

Figure 5. Influence of the concentration of alkali hydroxide vapor on the NO reduction rate: (●) only KOH releases, (■) only NaOH releases, and (★) both KOH and NaOH release and the concentration ratio of NaOH/KOH is 1.

and $C_{2,NO}$ is the NO emission concentration in the presence of alkali metal vapor. Figure 5 shows the influences of the concentrations of alkali hydroxide vapors on the NO reduction rate, and it indicates that the NO reduction rate increases with the increase of concentrations of alkali hydroxide vapors. When KOH and NaOH are separately present, NaOH can more effectively enhance the NO reduction rate, as compared to KOH. When KOH and NaOH are simultaneously present, the NO reduction rate slightly increases on the basis of that of NaOH. Thereby, the effect of NaOH on NO reduction is much greater than that of KOH.

Figure 6 shows the variations of gaseous composition concentrations with the reaction time in the presence of KOH (20 ppm) and NaOH (20 ppm) vapors during biomass reburning at T = 1700 K. NaOH makes the NO concentration noticeably decrease with the reaction time, as compared to KOH, and the concentrations of OH, H, NH_2, and NH are much lower at t = 0−0.04 s and higher at t = 0.04−0.4 s (see Figure 6). The modeling results indicate that NaOH can effectively inhibit H and OH formation at the beginning stage and subsequently promote H and OH formation at the later stage, and this is conducive to NO reduction. KOH can slightly control the free-radical concentration of H and OH at the whole stage.

The presence of alkali metal hydroxide vapors during reburning influences free-radical concentrations and t NO ROP, and the top seven NO production rates of reactions are presented in Figure 7. Because NO production rates of reactions are very stable and approach constants at t > 0.1 s, NO ROP is not provided at t = 0.1−0.4 s in Figure 7. A comparison of Figures 1 and 7 indicates that, in the presence of NaOH, NO ROPs are noticeably inhibited at the beginning stage, NO ROPs of reactions approach 0, expect for that of R5 ($NH_2 + NO = N_2 + H_2O$), which keeps a negative constant for NO reduction at t > 0.04 s, and R5 is the most important reaction for NO reduction in the whole reaction process. In the presence of KOH, NO ROPs are slightly inhibited at the beginning stage but the difference of NO ROPs of reactions in Figures 1 and 7b is little at t > 0.04 s.

To analyze NO reduction pathways in the presence of alkali metal hydroxides, the reaction pathway diagrams for N-, Na-, and K-containing species at the beginning of biomass reburning (0.004 s) are illustrated in Figures 8 and 9. A comparison of Figures 3, 8, and 9 indicate that, in the presence of NaOH or KOH, the reaction pathways of N-containing species are similar to those in the absence of alkali metals. NO-Reducing agents

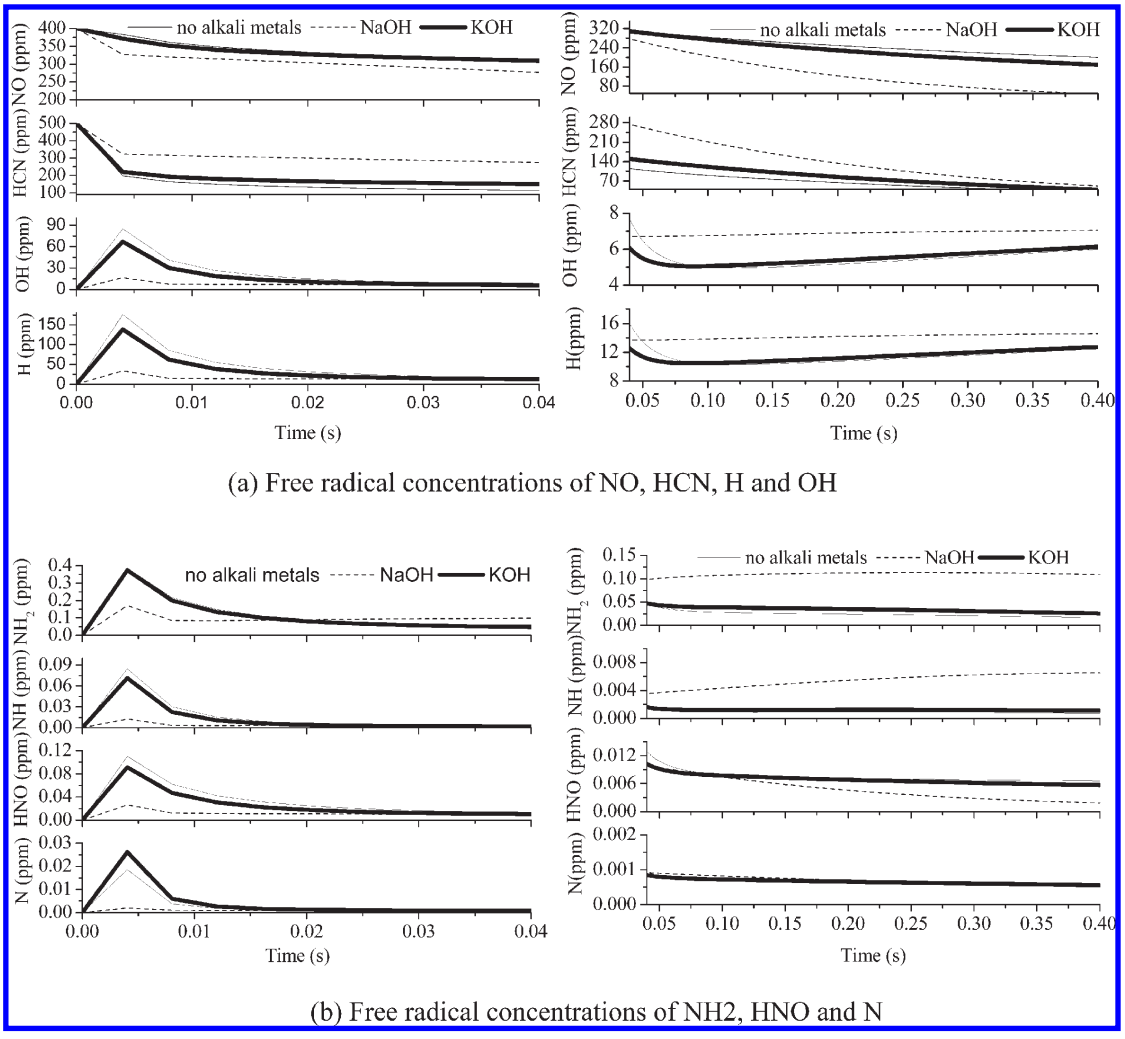

Figure 6. Variations of gaseous composition concentrations with the reaction time in the presence of KOH and NaOH vapors (initial concentration of 20 ppm): (a) free-radical concentrations of NO, HCN, H, and OH and (b) free-radical concentrations of NH_2, HNO, and N.

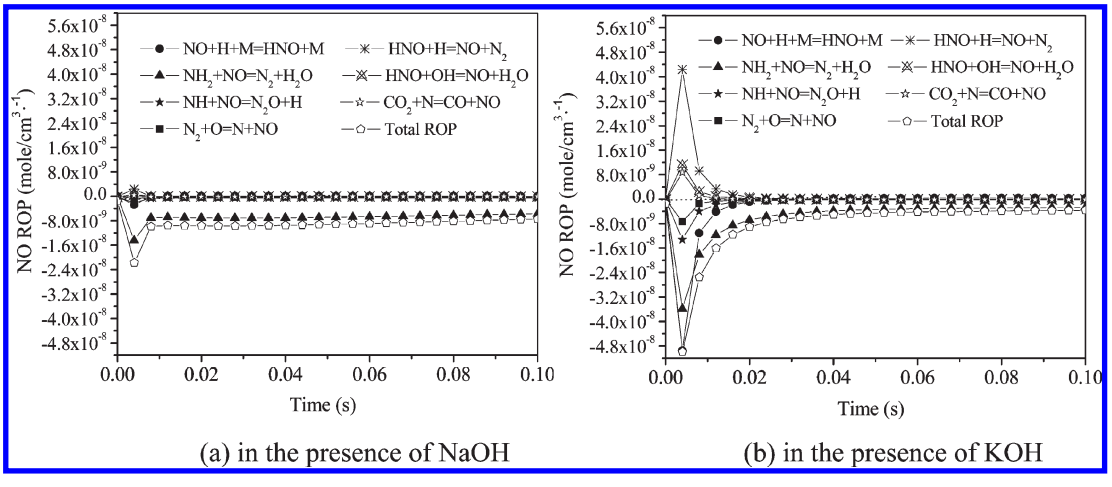

Figure 7. NO ROP versus the reactor time in the presence of KOH and NaOH (initial concentration of 20 ppm): (a) in the presence of NaOH and (b) in the presence of KOH.

(NH_2, NH, and N) derive from HCN, and HCN plays a critical role in NO reduction. In the presence of NaOH and KOH, the contributions of NH_2 for NO reduction are 93 and 71%, respectively. The difference is because the concentrations of H and OH in the presence of NaOH are lower than that in the presence of KOH (see Figure 6). The low concentrations of H

dx.doi.org/10.1021/ef200661x |*Energy Fuels* 2011, 25, 3465–3475

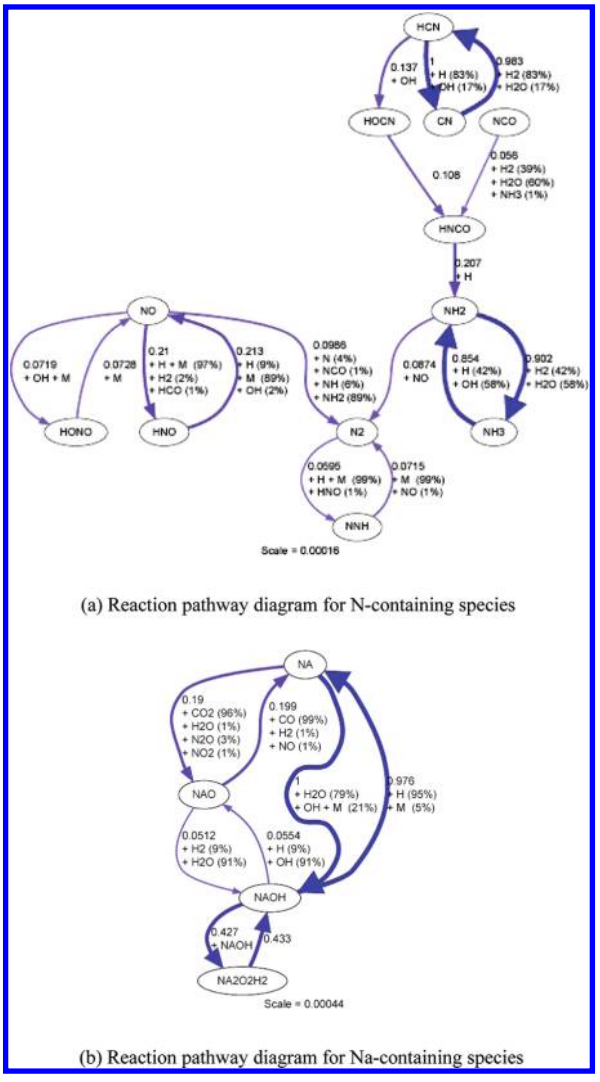

Figure 8. Reaction pathway diagrams for N- and Na-containing species in the presence of NaOH (initial concentration of 20 ppm) at $t = 0.004$ s: (a) reaction pathway diagram for N-containing species and (b) reaction pathway diagram for Na-containing species.

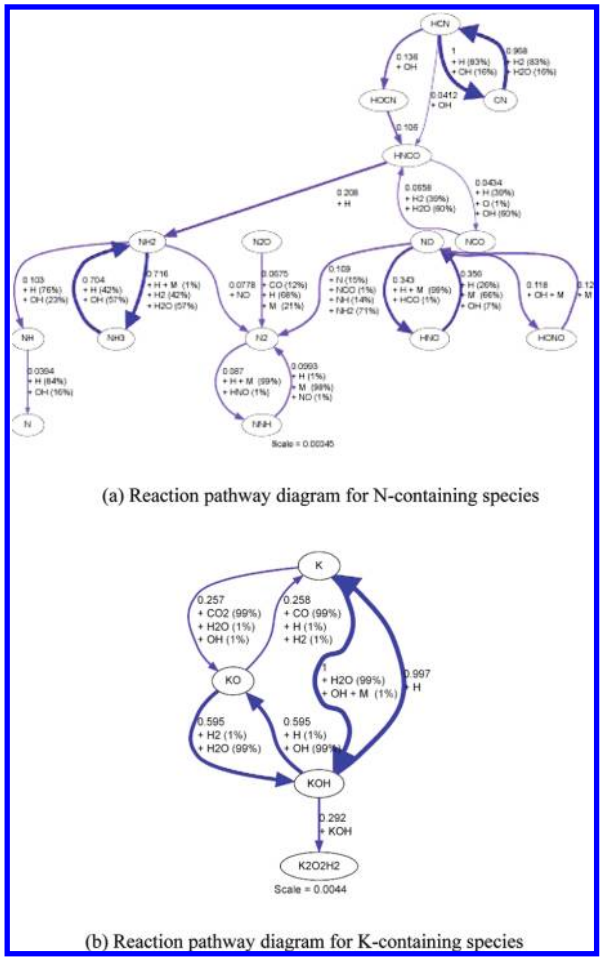

Figure 9. Reaction pathway diagrams for N- and K-containing species in the presence of KOH (initial concentration of 20 ppm) at $t = 0.004$ s: (a) reaction pathway diagram for N-containing species and (b) reaction pathway diagram for K-containing species.

and OH are not conducive to the conversion of NH_2 into NH and N, and thus, NH_2 has a higher contribution for NO reduction in the presence NaOH at the beginning stage of biomass reburning.

At the later stage, the reaction pathway diagrams for N-containing species are similar to those at the beginning of biomass reburning (0.004 s) and, thus, the reaction pathway diagrams are not presented. In the presence of NaOH, the contribution of NH_2 for NO reduction increases from 89 to 93% at t = 0.004−0.032 s and keeps constant (93%) at t = 0.032−0.4 s. In the presence of KOH, the contribution of NH_2 for NO reduction increases from 71 to 90% at $t = 0.004$−0.02 s and keeps constant (90%) at t = 0.02−0.4 s. In the presence of KOH, because HCN is significantly consumed at the beginning stage, the concentrations of NO reduction agents (NH_2 and NH) are low at a later stage of the reaction (see Figure 6), and this makes NO reduction difficult. In the presence of NaOH, because HCN is not significantly consumed at the beginning stage, the concentrations of NO-reducing agents (NH_2 and NH) are relative high at a later stage of the reaction (see Figure 6), and this then makes NO reduction easy.

Therefore, NO reduction strongly depends upon the local combustion environment, and the free-radical concentrations of H and OH influence NO reduction during biomass reburning. In the beginning stage, the concentration of the reburning fuel is high, its reaction with oxygen forms a large radical pool, the radicals initiate a rapid reaction between HCN and NO, HCN is rapidly depleted, and this is not conducive to NO reduction at a later stage.

Vitali et al.[36,37] have researched the effect of sodium salt on NO formation in combustion. The presence of alkali vapors tends to reduce the radical pool in the combustion system, and Na and K present "remove" the active oxidation species (OH and H) and inhabit NO formation.[38] The same behaviors were encountered experimentally and discussed by Zamansky et al.[12] In Figure 8b, the reactions of Na and NaOH at high temperatures (1700 K) consume H and OH radicals by the following reactions:

$$NaOH + H \rightarrow Na + H_2O \quad \text{(R18)}$$

$$Na + OH \rightarrow NaOH \quad \text{(R19)}$$

$$NaOH + NaOH \rightarrow Na_2O_2H_2 \quad \text{(R20)}$$

The net effect of R18 and R19 is the recombination of active species (H + OH = H_2O). Figure 10 shows the variations

dx.doi.org/10.1021/ef200661x |*Energy Fuels* 2011, 25, 3465–3475

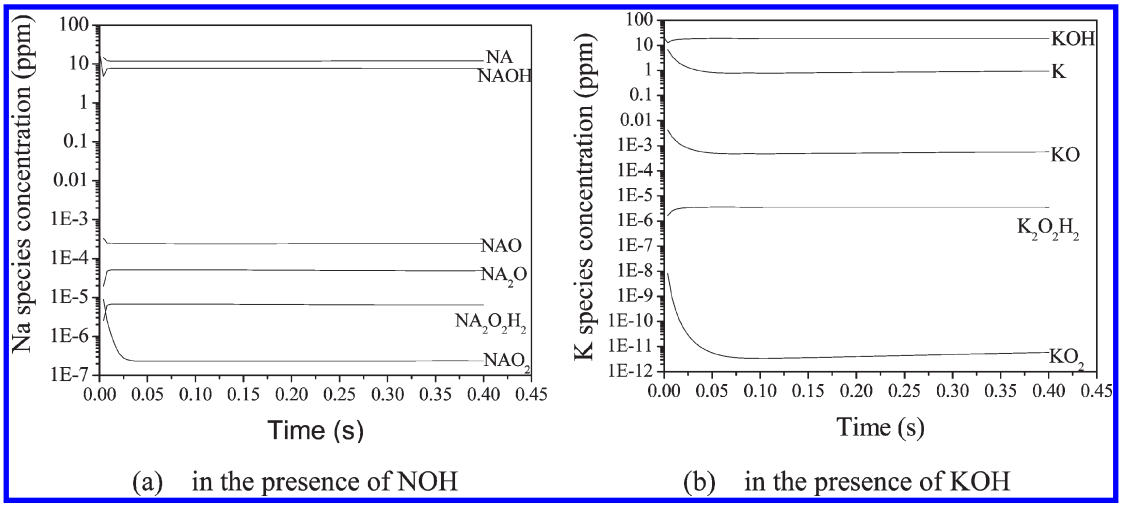

Figure 10. Variations of Na- and K-containing species concentrations with the reaction time in the presence of NaOH and KOH (initial concentration of 20 ppm): (a) in the presence of NOH and (b) in the presence of KOH.

of Na- and K-containing species concentrations with the reaction time. It indicates that the concentrations of NaOH and Na are higher than that of Na_2O, NaO_2, and $Na_2O_2H_2$, and then the reaction path of Na (NaOH → Na → NaOH) controls the concentrations of H and OH to affect NO reduction (see Figure 8b).

At the beginning stage of biomass reburning, the concentrations of H and OH are in super-equilibrium and it is 2 orders of magnitude greater than its equilibrium value without the release of alkali metals (see Figure 6a). The presence of NaOH can effectively control the free-radical concentrations of H and OH to low levels (see Figure 6a). This reduces the formation of NO-reducing agents (NH_2, NH, and N) by R1, R2, R6, R7, R9, and R10, and thus, the NO reduction rate of R5 slightly decreases, as compared to Figures 1 and 7a. In the meantime, the presence of NaOH can inhibit the conversion of HCN into NH, HNO, and N because of low concentrations of H and OH, and this avoids the NO formation through the consumption of a large amount of HCN by R13 and R17 at the beginning stage of biomass reburning.

At the later stage of biomass reburning, the concentrations of H and OH reach low-level equilibrium, an increase of the concentration of H and OH is conducive to the conversion of HCN into NH_2, and NO is reduced to N_2 by the reaction pathway HCN → HOCH/HNCO → NH_2 + NO → N_2 + H_2O. The presence of NaOH can make the concentrations of H and OH sustain relatively high levels by the reaction path of Na (NaOH → Na → NaOH) (see Figure 8b). HCN is kept sufficient for NO reduction (see Figure 6a) because of the low consumption of HCN at the reaction beginning stage.

xIn other words, during biomass reburning, the reactions of Na-containing species can sustain the relative high rates of NO reduction by controlling the free-radical concentrations of H and OH, and thus, Na-containing species is very important for NO reduction.

In the meantime, Na species can process following reaction

$$Na + N_2O \rightarrow NaO + N_2 \quad \text{(R21)}$$

$$NaO + CO \rightarrow Na + CO_2 \quad \text{(R22)}$$

$$net: N_2O + CO \rightarrow N_2 + CO_2$$

The net effect of R21 and R22 is that N_2O is destroyed to form N_2.

As known from Figures 8b and 9b, the behavior of K-containing species is similar to that of Na-containing species, and the similar behaviors of Na- and K-containing species were found experimentally by Zamansky et al.[12] The concentrations of K and KOH are high in Figure 10b, and the main reaction pathways of K-containing species in Figure 9b are as follows:

$$KOH + H \rightarrow K + H_2O \quad \text{(R23)}$$

$$K + OH \rightarrow KOH \quad \text{(R24)}$$

$$K + H_2O \rightarrow KOH + H \quad \text{(R25)}$$

Figure 9b indicates that R25 predominates in KOH formation and R24 is negligible. In the reaction pathways of NaOH → Na → NaOH and KOH → K → KOH, the reaction rate constants of R18 and R23 are equal but the reaction rate constant of R24 is only $^1/_{647}$ of R19. R24 limits the cycle reactions of KOH → K → KOH. A high concentration of free radicals of H and OH cannot be effectively removed at the beginning time (see Figure 6a), and then, a large amount of HCN is finally conversed into NO by R12−R17. At the later stage, because of the low concentration of H, OH, and HCN, NO reduction is difficult. Thereby, during biomass reburning, KOH has less influence on NO reduction than NaOH.

4.3. NO Reduction by the Release of Alkali Metal Chlorides. It is assumed that K and Na species can be released in the vapor forms of hydroxides (NaCl and KCl), and both NaCl and KCl concentrations are 20 ppm. The modeling results indicate that the influence of NaCl and KCl on the NO reduction rate is the same as that of NaOH and KOH (see Figure 5), and the influence of the concentration of alkali chloride vapors on the NO reduction rate is not provided.

Here, the concentrations of Na- and K-containing species are presented in Figure 11. In Figure 11a, the concentrations of Na, NaCl, and NaOH are high. The result indicates that the reactions involving Na, NaCl, and NaOH species are

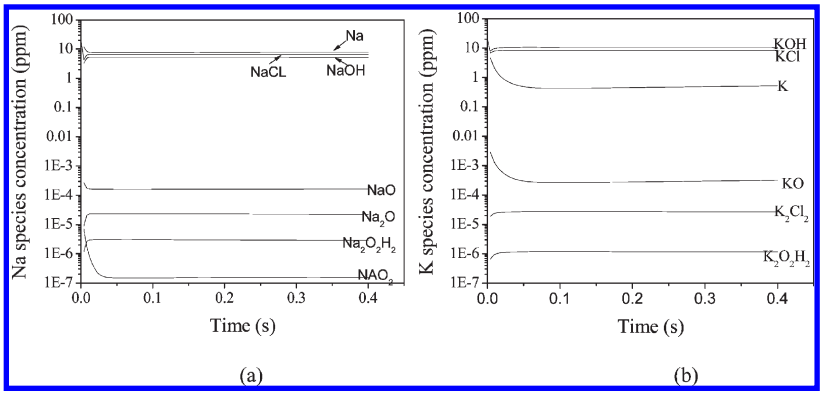

Figure 11. Variations of Na- and K-containing species concentrations with the reaction time in the presence of KOH and NaOH (initial concentration of 20 ppm).

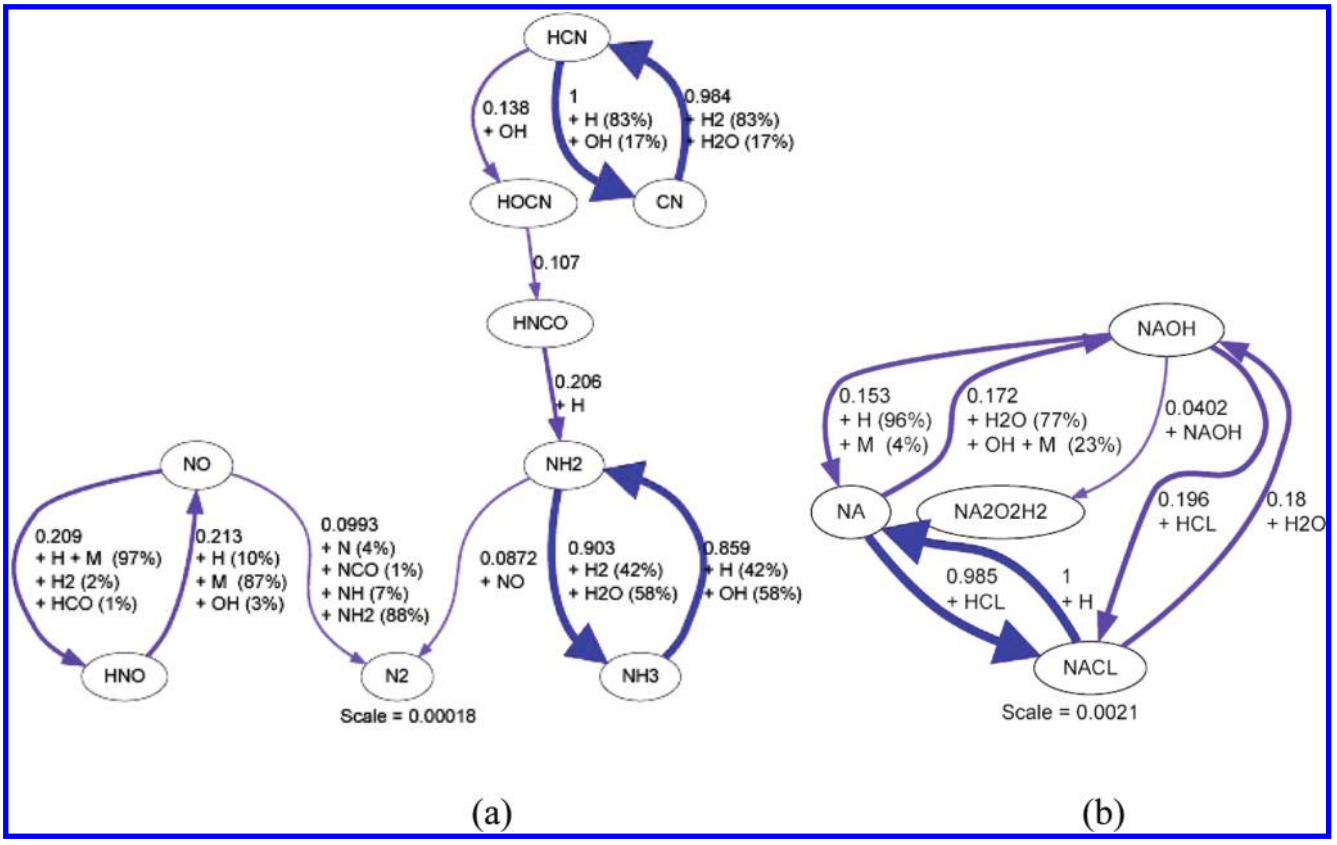

Figure 12. Reaction pathway diagrams for N- and Na-containing species in the presence of NaCl during biomass reburning at t = 0.004 s.

dominant in Na-containing reactions, and these important reaction pathways are shown in Figure 12b.

$$NaCl + H_2O = NaOH + HCl \quad (R26)$$

$$NaCl + H = Na + HCl \quad (R27)$$

$$NaOH + H = Na + H_2O \quad (R28)$$

$$NaOH + M = Na + OH + M \quad (R29)$$

Figure 12 shows the reaction pathway diagrams for N- and Na-containing species in the presence of NaCl during biomass reburning at t = 0.004 s. When Figure 8a is compared to Figure 12a, in the presence of NaOH and NaCl during biomass reburning, the reaction pathways of N-containing species are similar and the contributions of NO-reducing agents (NH_2, NH, and N) for NO reduction are nearly identical. Although HCl is formed through R26 and R27, Figure 12a indicates that the reaction pathways of N-containing species are not influenced by HCl during biomass reburning and HCl formation has no influence on NO emission. Experiments by Wei et al.[39] also found that HCl addition has almost no influence on NO_x emissions under fuel-rich combustion conditions.

In the presence of KCl, the reaction pathway of N-containing species is the same as that in the presence of KOH (see

dx.doi.org/10.1021/ef200661x |*Energy Fuels* 2011, 25, 3465–3475

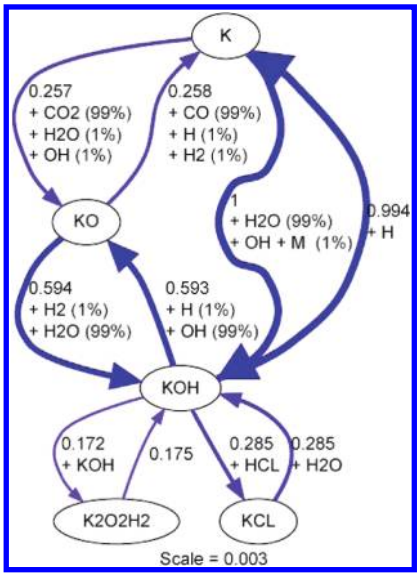

Figure 13. Reaction pathway diagram for K-containing species in the presence of KCl (initial concentration of 20 ppm).

Figure 9a); thus, the pathway is not provided. Figure 13 shows the reaction pathway of K-containing species. In Figure 11b, the concentrations of KOH, KCl, and K are high. The reactions involving species KOH, KCl, and K are dominant in K-containing reactions, and these important reaction pathways in Figure 13 are as follows:

$$KCl + H_2O = KOH + HCl \quad (R30)$$

$$KOH + H = K + H_2O \quad (R31)$$

5. CONCLUSION

Biomass reburning was simulated using the Sandia SENKIN program, and the promotion mechanism of NO reduction by K- and Na-containing species vapor released from biomass was investigated. Na-Containing species have great promotion of NO reduction by controlling the free radicals of H and OH, as compared to K-containing species, and the effects of alkali metal hydroxide vapors and alkali metal chloride vapors on the NO reduction rate were identical. At the beginning stage of biomass reburning, Na-containing species can effectively inhibit the conversion of HCN into NH, HNO, and N by controlling the formation of H and OH and it avoids NO formation. At the later stage of biomass reburning, the free-radical levels of H and OH reach equilibrium, Na-containing species can promote the formation of H and OH to sustain a relatively high level through the chemical reaction path of NaOH → Na → NaOH, and NO is effectively reduced. Because the reaction rate constant of K + OH = KOH is only $^1/_{64}$ of Na + OH = NaOH, KOH has low promotion of NO reduction, as compared to NaOH.

AUTHOR INFORMATION

Corresponding Author

*Telephone/Fax: +86-10-82544231. E-mail: lisen@imechac.cn.

ACKNOWLEDGMENT

Financial support by the National Natural Science Foundation of China (50976123 and 50776099) and the Knowledge Innovation Program of the Chinese Academy of Sciences (KGCX2-YW-321) is acknowledged.

REFERENCES

(1) Li, S.; Xu, T. M.; Zhou, Q. L.; Tan, H. Z.; Hui, S E.; Hu, H. L. *Fuel* **2007**, *86*, 1169–1175.

(2) Hald, P. *Prepr. Pap.—Am. Chem. Soc., Div. Fuel Chem.* **1995**, *40*, 753–757.

(3) Dayton, D. C.; French, R. J.; Milne, T. A. *Energy Fuels* **1995**, *9*, 855–865.

(4) Zamansky, V. M.; Sheldon, M. S.; Lissianski, V. V.; Maly, P. M.; Moyeda, D. K.; Marquez, A.; Seeker, W. R. *Advanced Biomass Reburning for High Efficiency NO_x Control*; GE Energy and Environmental Research Corporation: Irvine, CA, 2000; Department of Energy (DOE), National Energy Technology Laboratory (NETL) Contract DE-FC26-97FT-97270.

(5) Lissianski, V. V.; Zamansky, V. M.; Maly, P. M. *Biomass Reburning—Modelling/Engineering*; GE Energy and Environmental Research Corporation: Irvine, CA, 1999; Department of Energy (DOE), National Energy Technology Laboratory (NETL) Contract DE-FC26-97FT-97270.

(6) Munir, S.; Nimmo, W.; Gibbs, B. M. *J. Qual. Technol. Manage.* **2010**, *6*, 43–79.

(7) Nimmo, W.; Liu, H. Developments in NO_x emission control by reburning in pulverised coal combustion. In *Coal Combustion Research*; Grace, C. T., Ed.; Nova Science Publishers, Inc.: Hauppauge, NY, 2010; pp 85−170.

(8) Nimmo, W.; Singh, S.; Gibbs, B. M.; Williams, P. T. *Fuel* **2008**, *87*, 2893–2900.

(9) Hampartsoumian, E.; Folayan, O. O.; Nimmo, W.; Gibbs, B. M. *Fuel* **2003**, *82*, 373–384.

(10) Nimmo, W.; Patsias, A. A.; Hall, W.; Williams, P. T. *Ind. Eng. Chem. Res.* **2005**, *44*, 4484–4494.

(11) Ballester, J.; Ichaso, R.; Pina, A.; González, M. A.; Jiménez, S. *Biomass Bioenergy* **2008**, *32*, 959–970.

(12) Zamansky, V. B.; Ho, L.; Maly, P. M.; Seeker, W. R. *Proc. Combust. Inst.* **1996**, *26*, 2075–2082.

(13) Lee, S.; Park, K.; Park, J. W.; Kim, B. H. *Combust. Flame* **2005**, *141*, 200–203.

(14) Liu, Y. H.; Liu, Y. H.; Che, D. F.; Xu, T. M. *Proc. Chin. Soc. Electr. Eng.* **2005**, *25*, 136–141.

(15) Avelina, G. G.; María, J. I. G.; Angel, L. S.; Concepción, S. M. L. *Fuel* **1997**, *76*, 499–505.

(16) Sjaak, V. L.; Jaap, K. *The Handbook of Biomass Combustion and Co-firing*; EarthScan: Oxford, U.K., 2008.

(17) Dayton, D. G.; Milne, T. A. *Proceedings of the 21th National Meeting of the American Chemical Society, Division of Fuel Chemistry*; Chicago, IL, 1995; pp 758−762.

(18) Chenevert, B. C.; Kramlich, J. C.; Nichols, K. M. *Proc. Combust. Inst.* **1999**, *27*, 1719–1725.

(19) Sandia National Laboratories. *SENKIN: A Fortran Program for Predicting Homogeneous Gas Phase Chemical Kinetics with Sensitivity Analysis*; Sandia National Laboratories: Livermore, CA, 1988; SAND87-8248.

(20) Sandia National Laboratories. *CHEMKIN-II: A Fortran Chemical Kinetics Package for the Analysis of Gas Phase Chemical Kinetics*; Sandia National Laboratories: Livermore, CA, 1989; SAND89-8009B.

(21) *Cantera: Object-Oriented Software for Reacting Flows*; http://www.cantera.org.

(22) Dagaut, P.; Lecomte, F.; Chevailler, S.; Cathonnet, M. *Combust. Sci. Technol.* **1998**, *139*, 329–363.

(23) Dagaut, P.; Lecomte, F.; Chevailler, S.; Cathonnet, M. *Combust. Flame* **1999**, *119*, 494–504.

(24) Dagaut, P.; Luche, J.; Cathonnet, M. *Proc. Combust. Inst.* **2000**, *28*, 2459–2465.

(25) Dagaut, P.; Lecomte, F. *Energy Fuels* **2003**, *17*, 608–613.

(26) Zamansky, V. M.; Maly, P. M.; Lissianski, V. V.; Sheldon, M. S.; Moyeda, D.; Payne, R. *Secondary Generation Advanced Reburning for High*

Efficiency NO_x Control; GE Energy and Environmental Research Corporation: Irvine, CA, 2001; DOE Contract DE-AC22-95PC95251.
(27) Glarborg, P.; Marshall, P. *Combust. Flame* **2005**, *141*, 22–39.
(28) Hindiyarti, L.; Frandsen, F.; Livbjerg, H.; Glarborg, P.; Marshall, P. *Fuel* **2008**, *87*, 1591–1600.
(29) Dagaut, P.; Lecomte, F. *Fuel* **2003**, *82*, 1033–1040.
(30) Chen, Y.; Charpenay, S.; Jensen, A.; Wójtowicz, M. A.; Serio, M. A. *Proc. Combust. Inst.* **1999**, *27*, 1327–1334.
(31) Williams, A.; Pourkashanian, M.; Jones, J. M. *Proceedings of the 5th International Conference on Technologies and Combustion for a Clean Environment*; Lisbon, Portugal, 1999; pp 945−952.
(32) *Cantera: Object-Oriented Software for Reacting Flows*; http://www.cantera.org.
(33) Dryer, F. L.; Glassman, I. *Proceedings of the 14th International Symposium on Combustion*; The Combustion Institute: Pittsburgh, PA, 1973.
(34) Hardy, J. E.; Lyon, R. K. *Combust. Flame* **1980**, *39*, 317–320.
(35) El-Mahallawy, F.; E-Din Habik, S. *Fundamentals and Technology of Combustion*; Elsevier Science: Amsterdam, The Netherlands, 2002.
(36) Yang, W.; Zhou, J.; Liu, M.; Zhou, Z.; Liu, J.; Cen, K. *Energy Fuels* **2007**, *21*, 2548–2554.
(37) Lissianski, V. V.; Zamansky, V. M.; Maly, P. M. *Combust. Flame* **2001**, *125*, 1118–1127.
(38) Carucci, J. R. H.; Kilpinen, P. *Turk. J. Eng. Environ. Sci.* **2006**, *30*, 163–174.
(39) Wei, X. L.; Han, X. H.; Schnell, U.; Maier, J.; Worner, H.; Hein, K. R. G. *Energy Fuels* **2003**, *17*, 1392–1398.